Electronic Supplementary Information: Applications of the density functional method combined with the electron-positron correlation-polarization potential to positron binding to hydrocarbons and water clusters

Daisuke Yoshida,*[,†,‡] Toshiyuki Takayanagi,[¶] Yukiumi Kita,[‡] Tomomi Shimazaki,[‡] and Masanori Tachikawa[‡]

†*Department of Physics, Tohoku University, Aramaki Aza-Aoba 6-3, Aoba-ku, Sendai, Miyagi 980-8578, Japan.*

‡*Quantum Chemistry Division, Yokohama City University, Seto 22-2, Kanazawa-ku, Yokohama 236-0027, Japan*

¶*Department of Chemistry, Saitama University, Shimo-Okubo 255, Sakura-ku, Saitama, Saitama 338-8570, Japan*

E-mail: daisuke.yoshida.b1@tohoku.ac.jp

S1. Benchmark calculations for electron-positron LDA functionals

We show benchmark calculations using the different electron-positron correlation functional $V_{\rm corr}^{\rm LDA}(\boldsymbol{r})$ in Eq. (3). In the main paper, we have used the LDA functional proposed by

Boroński and Nieminen (BN)[S1] (see the main text for details) with the aim of at comparing the present modification for CPP with the previous version that employed the BN functional in earlier studies. Meanwhile the latest LDA functional developed by Drummond *et al.* (hereafter referred to as DLNP) based on diffusion Monte Carlo combined with the Slater-Jastrow-Backflow trial wavefunctions,[S2] is also available. The DLNP correlation energy $V_{\rm corr}(r_s)$ (in atomic units) is represented by the following single formula (as a function of the density parameter r_s),

$$V_{\rm corr}^{\rm DLNP}(\boldsymbol{r}_p) = \frac{A_{-1}{r_s}^{-1} + A_0 + A_1 r_s - 0.262005 B_2 {r_s}^2}{1 + B_1 r_s + B_2 {r_s}^2}, \tag{1}$$

where $A_{-1} = 0.260361$, $A_0 = -0.261762$, $A_1 = 0.00375534$, $B_1 = 0.113718$, and $B_2 = 0.0270912$. This function asymptotically reproduces the correct low-density energy limit of the positronium negative ion Ps^- (i.e., approximately 0.262 Ha), similarly to the BN functional in Eq. (4) presented in the main text. As shown in Figure S1, where the correlation energies are plotted against the density parameter r_s, the DLNP functional shows only small differences from the LDA functional (within 0.02 Ha) in the range of $r_s < 3$ bohr. However, the difference increases as r_s becomes larger (in the low electron density region). These differences suggest that the tendency of LDA to overestimate the correlation energy is somewhat suppressed compared to the BN functional.

Table S1 shows the calculation results by the DFT-CPP method at GGA level with the DLNP functional[S2] for the positron affinity PA of $C_{10}H_{22}$. Under the same computational conditions with the main paper, where the gradient correction parameter $\beta = 0.38$ is applied, the accurate DLNP functional gives a PA value approximately 30-40 % smaller than that obtained by using the BN functional, as well as the experimentally measured value. By applying some GGA-β parameter, we have found that slightly smaller values of $\beta = 0.34$–0.35 yield reasonable PA values. The benchmark results demonstrate the applicability of the DLNP correlation energy to positronic complexes in finite size systems.

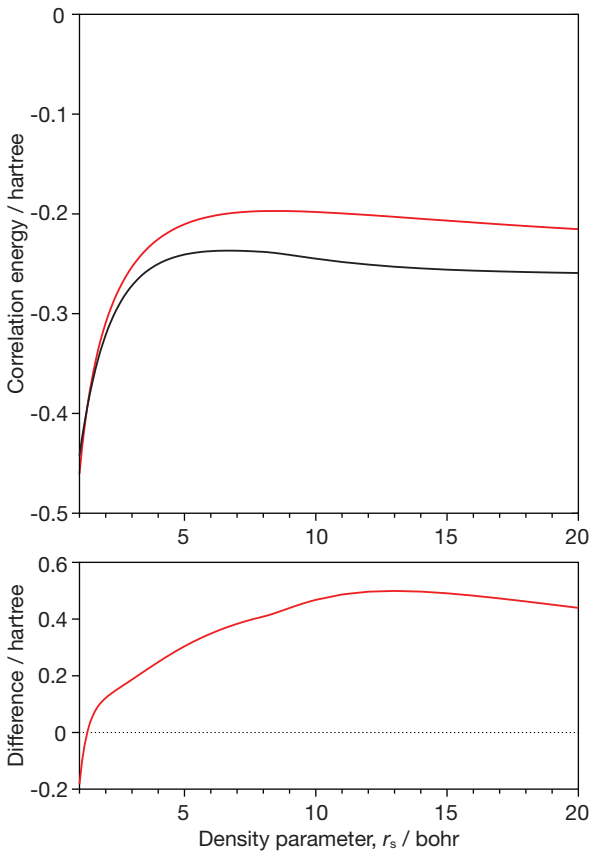

Figure S1: Comparison of the BN (black) and DLNP (red) correlation functionals, $V_{\rm corr}^{\rm BN}$ and $V_{\rm corr}^{\rm DLNP}$. The bottom figure shows the difference of these correlation energies, $V_{\rm corr}^{\rm DLNP} - V_{\rm corr}^{\rm BN}$.

Table S1: Calculation results by DFT-CPP with the DLNP functional combined with GGA corrections for the positron affinity PA of $C_{10}H_{22}$. PAs are given in units of meV.

β	PA
0.34	198.7
0.35	175.6
0.38	113.4

S2. Test calculations

We present test calculations for determining computational conditions employed in this work. All test calculations are carried out by using the DFT-CPP with the GGA correction with the $\beta = 0.38$, where the electronic structure for $C_{10}H_{22}$ obtained at the ωB97X-D/aug-cc-pVDZ level are used. The other computational conditions are also set to the same values as those presented in the main text; the length of the box size are $140a_0$ bohr (with the Bohr radius a_0) and the number of grid points is 512 for each coordinate. The relaxation calculations are achieved in the energy convergence criterion of 1×10^{-9}. Table S2 shows the positron energies calculated with different four energy cutoffs, $E_{\rm cut} = 5$, 10, 20, and 30 Ha. Within this range, the results are not significantly affected by the cutoff criterion when $E_{\rm cut} \geq 10$ Ha; threfore, we employed $E_{\rm cut} = 20$ Ha ~ 540 eV. All subsequent benchmark data were obtained by using this cutoff energy.

Table S2: Calculation results for different cutoff energies. The cutoff energies $E_{\rm cut}$ and positron affinities PAs are shown in units of Ha and meV, respectively.

$E_{\rm cut}$	PA
5	197.1
10	192.4
20	191.6
30	191.5

Next, we provide the calculation results obtained by employing different box sizes and grid points. One of the aims of this study is to establish an efficient and practical approach that is universally applicable for large-scale molecular systems. To this end, it is necessary to find reasonable computational conditions tentatively applied to a wide range of molecular size. Especially for large alkanes, $V(\boldsymbol{r})$ still has finite values of $\sim 10^{-6}$ a.u. at the boundary regions for $L \sim 80a_0$–$100a_0$, while $V(\boldsymbol{r})$ converges to $\sim 10^{-7}$–10^{-8} at the boundary regions for larger L. Based on these numerical criteria, this time we adopted the box size with $L = 140a_0$ for most of the species presented in this work, which is sufficiently large to ensure

that the effective potential converges asymptotically at the boundary surfaces. As for the grid size, we examined the dependence of calculated positron affinities on the number of grid points. The results are shown in Table S3 and an example of the plot as a function of the grid points for $L = 140a_0$ is given in Figure S2. For t-$C_{10}H_{22}$, the experimental value of PA is 193 meV, while the grid intervals smaller than $0.2a_0$–$0.3a_0$ yield PA values within the accuracy of approximately 5 % deviation, which is considered acceptable accuracy. In Figure S2, the saturation behavior can be found in grids of $M \gtrsim 500$. These small deviations in positron affinities can be compensated by slightly tuning the gradient correction parameter, β in Eq. (3). Although this procedure is also somewhat empirical, we confirmed that the variation in the β parameter is very small; for example, applying $\beta = 0.38$–0.39 yields reasonable positron affinities, instead of $\beta = 0.38$ presented in the main body of the paper.

Table S3: Positron affinities calculated with the different quadrature grids. Both the box length L and grid interval L/M (with the number of grid point for each coordinate, M) are given in atomic units, and the positron affinity PA $= -\varepsilon_{\mathrm{p}}$ is given in units of meV.

L	M	L/M	PA	
			$\beta = 0.38$	$\beta = 0.39$
140	640	0.218	205.6	183.7
140	512	0.273	191.6	–
140	384	0.364	163.7	–
140	256	0.546	95.3	–
100	640	0.156	216.0	194.0
100	576	0.173	213.8	–
100	512	0.195	209.6	187.6
100	480	0.208	208.6	–
100	384	0.260	193.8	–
100	256	0.390	148.2	–
80	512	0.156	216.1	–
80	320	0.250	197.5	–
80	256	0.312	181.9	–

Furthermore, we have also examined the positron affinity of the water dimer $(H_2O)_2$. A previous study employing *ab initio* large-scale CI calculations reported a PA of approximately 38 meV for $(H_2O)_2$, while the present calculation provided a consistent value of approximately

35 meV, as shown in the main text. Based on above benchmark results and considering the computational cost, we have employed the grid size of $(512)^3$, which provides the necessary level of accuracy for the scope of this study.

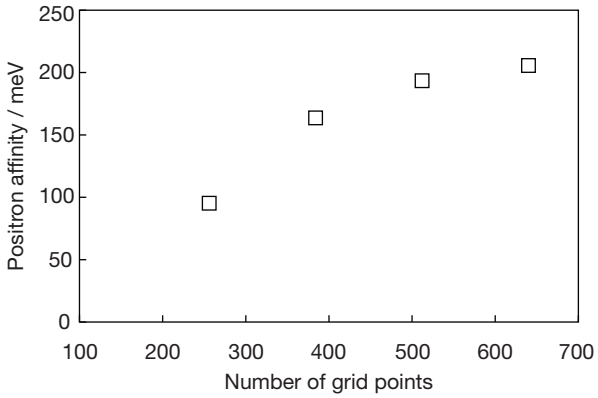

Figure S2: Dependence of the calculated positron affinities on the quadrature grids. The calculations were performed for the $[C_{10}H_{22}; e^+]$ system at a space with the length of $L = 140a_0$.

S3. Structure data

A ZIP archive file named structure_xyz.zip is provided as part of the ESI. It contains Cartesian coordinates in .xyz format for all optimized geometries discussed in the main paper. Each file is named according to the molecular/cluster system (see for the details of computational procedures), where the coordinates are given in standard XYZ format.

These optimized geometries were obtained by the procedures presented in Section 3 of the main paper. The final convergence of the geometry optimization was achieved with a maximum energy gradient of less than 4.5×10^{-4} a.u. and an self-consistent field energy threshold below 10^{10} hartree.

References

(S1) Boroński, E.; Nieminen, R. M. Electron-positron density-functional theory. *Phys. Rev. B* **1986**, *34*, 3820.

(S2) Drummond, N. D.; López Ríos, P.; Needs, R. J.; Pickard, C. J. Quantum Monte Carlo Study of a Positron in an Electron Gas. *Phys. Rev. Lett.* **2011**, *107*, 207402.